# Complex domain nonlocal group-wise sparsity: toward wavelength super-resolution phase imaging in coherent optics

Vladimir Katkovnik and Karen Egiazarian
Signal Processing Laboratory, Tampere University of Technology, Tampere, Finland
Email: vladimir.katkovnik@tut.fi, karen.egiazarian@tut.fi

Phase imaging is one of the key instruments in coherent optics to make visible features of specimens, which are nearly invisible in the conventional light microscopy, and produce precise high resolution measurements (e.g. [1]- [3]). It is possible due to a high phase sensitivity to variations in shape, refraction index and internal structure of specimens. While only intensity of the light field can be measured, visualization of phase from intensity observations is an important problem. In the phase contrast microscopy, the wavefront modulation in the Fourier plane was used in order to resolve this problem. Despite the revolutionary success of these methods only *qualitative visualization* of phase can be achieved in this way, where the features of specimens even visible maybe be so distorted that accurate measurements and even a proper interpretations can be problematic.

*Quantitative visualization* is targeted on direct phase imaging and precise measurements. In the modern development the quantitative phase imaging is fundamentally based on digital data processing.

Let us consider the following formalization of the phase retrieval problem:

$$y_s = |\mathcal{P}_s\{u_o\}|^2,\ s = 1, ..., L, \tag{1}$$

where: $u_o \in \mathbb{C}^{N\times N}$ is an $N \times N$ complex-valued object (specimen); $\mathcal{P}_s$: $\mathbb{C}^{N\times N} \longmapsto \mathbb{C}^{M\times M}$ is a complex-valued operator of the wavefront propagation from the object to sensor planes, $y_s \in \mathbb{R}_+^{M\times M}$ is an $M \times M$ intensity observations of the wavefronts at the sensor plane. For the noisy data $z_s = \mathcal{G}\{|u_s|^2\}$, $s = 1, ..., L$, where $\mathcal{G}$ stands for a generator of random observations, the noisy $\{z_s\}$ are used instead of $\{y_s\}$.

In the optical setup shown in Fig.1 the forward propagation operator $\mathcal{P}_s\{u_o\}$ linking the object and sensor wavefronts, $u_o$ and $u_s$, is of the form

$$u_s(\xi, \eta) = \mu \exp\{j\frac{\pi}{\lambda f}(\xi^2 + \eta^2)\}\mathcal{F}_{u_o\cdot\mathcal{M}_s}(\xi/\lambda f, \eta/\lambda f), \tag{2}$$

where $\mathcal{F}_{u_o\cdot\mathcal{M}}$ is the Fourier transform of the product $u_o(x, y)\mathcal{M}_s(x, y)$, $\mathcal{M}_s(x, y)$ is a complex valued transmission function of the phase modulation mask, $\lambda$ is a wavelength and $f$ is a focal length of the lens.

Reconstruction of the complex-valued object $u_o = a_o \exp(i\varphi_o)$ from noiseless $\{y_s\}$ or noisy observations $\{z_s\}$ is *phase retrieval problem*. Here *phase* emphasizes that in the object the phase is a variable of the first priority, while the amplitude may be treated as an auxiliary variable often useful only in order to improve the phase reconstruction.

The sparse representation can be imposed on complex-valued $u_o$ directly using complex-valued basic functions or on the following pairs of real-valued variables :

(1) The phase $\varphi$ (interferometric or absolute) and the amplitude $B_o$;

(2) The real and imaginary parts of $u_o$.

In what follows, we use the sparsity imposed on the phase and the amplitude. The variational formulation of the phase retrieval optimal for noisy data results in the likelihood criterion and optimization with the sparsity constraints. It has been shown in a number of works for various optical problems (e.g. [5]-[6]) that the algorithms are iterative and the nonlocal group-wise sparsity is implemented as the BM3D filtering applied separately to phase and amplitude updates.

The phase retrieval for the considered problem provided Poissonian noisy observations can be formalized as the Nash equilibrium balancing on $(\{\mathbf{u}_s\}_1^L, \mathbf{u}_o, \boldsymbol{\theta}_a, \boldsymbol{\theta}_\varphi)$ of two criteria [7]:

$$\mathcal{L}_1(\{\mathbf{u}_s\}, \mathbf{u}_o) = \sum_{s=1}^{L}\sum_{l=1}^{n}[|\mathbf{u}_s[l]|^2\chi - \mathbf{z}_s[l]\log(|\mathbf{u}_s[l]|^2\chi)] + \frac{1}{\gamma_1}\sum_{s=1}^{L}||\mathbf{u}_s - \mathcal{P}_s\{\mathbf{u}_o\}||_2^2, \tag{3}$$

$$\mathcal{L}_2(\boldsymbol{\theta}_\varphi, \boldsymbol{\theta}_a, \boldsymbol{\varphi}, \mathbf{a}) = \tau_a \cdot ||\boldsymbol{\theta}_a||_0 + \tau_\varphi \cdot ||\boldsymbol{\theta}_\varphi||_0 + \frac{1}{2}||\boldsymbol{\theta}_a - \Phi_a\mathbf{a}||_2^2 + \frac{1}{2}||\boldsymbol{\theta}_\varphi - \Phi_\varphi\boldsymbol{\varphi}||_2^2,\ \mathbf{u}_o = \mathbf{a} \circ \exp(j\boldsymbol{\varphi}). \tag{4}$$

Here the analysis $\Phi_a$ and synthesis $\Phi_\varphi$ frames are designed using BM3D technique, i.e. nonlocal group-wise sparsity, and $\boldsymbol{\theta}_a$ and $\boldsymbol{\theta}_\varphi$ are the respective spectral variables for the amplitude and the phase.

It is shown for this formalization that the BM3D sparsity results in the separate filtering of phase and amplitude of the form:

$$\hat{\boldsymbol{\varphi}} = BM3D_{phase}(\boldsymbol{\varphi}_{,}, th_\varphi), \hat{\mathbf{a}} = BM3D_{ampl}(a, th_B),$$

where BM3D stands for BM3D thresholding filtering.

Here *phase* and *ampl* as indices of BM3D are used in order to emphasize that the parameters of BM3D can be different for phase and amplitude. BM3D procedures update (filter) input superindices variables; $th_\varphi$ and $th_B$ are threshold parameters of the algorithms. This kind of phase/amplitude as well as real/imaginary parts sparsity modeling has been applied for a number of phase imaging problems (e.g. [5]-[8]). The complex domain sparsity targeted on the direct sparse approximations of $\mathbf{u}_o$ appeared in the recent works [4], [9]-[11].

The main contribution of this paper is a development of the super-resolution phase retrieval algorithm for the criteria (3)-(4 and the optical setup shown in Fig.1, where a random phase modulation is implemented by a spatial light modulators (SLM) located in the object plane. The simulation experiments (Figs. 2-6) demonstrate a good performance of the algorithm up to the super-resolution factor $r_s = 32$. For $r_s = 32$ the computational pixels are equal to $\lambda/4$, i.e. a sub-wavelength resolution is demonstrated.

**Acknowledgment**

This work is supported by Academy of Finland, project no. 287150, 2015-2019.

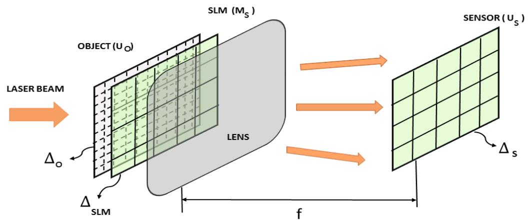


Fig. 1. Optical setup with a single lens for phase retrieval from modulated diffractive patterns: Object (o), Spatial light modulator (SLM), Lens and Sensor (s). The object is placed against the lens and the distance from the lens to the sensor is equal to the focal length of the lens $f$. The object, lens and spatial light modulator (SLM) shown between the object and lens are located in the same plane. In this consideration the object, SLM and lens are wavefront transformers for a uniform monochromatic normally incident plane wave (laser beam).

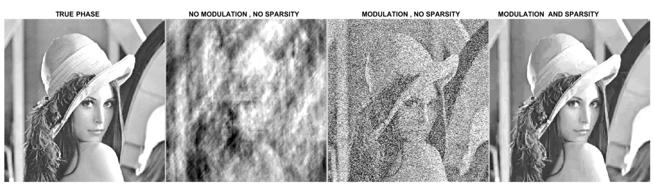


Fig. 2. Phase reconstructions, from left-to-right: (a) true lena image, (b) reconstruction without phase modulation, (c) reconstruction with phase modulation but without SPAR filtering, (d) reconstruction with phase modulation and with SPAR filtering, $L = 1$, $r_s = 1$.

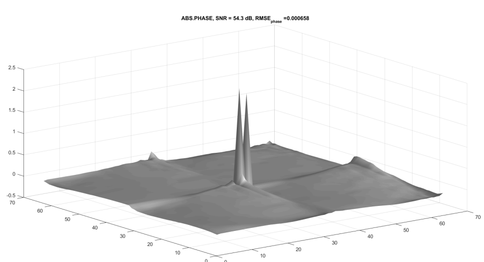

Fig. 3. 3D surfaces for sub-wavelength reconstruction of two phase-peak images, $r_s = 32$. The distance between the peaks is equal to 0.257 $\lambda$ . A sub-wavelength resolution is demonstrated.

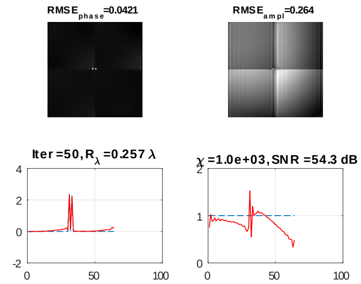


Fig. 4. Two-peaks reconstructions: distance between the phase peaks is equal to 0.257 $\lambda$, $r_s = 32$. Four 32 x 32 squares well seen in amplitude reconstructions correspond to the four pixels of SLM. The cross-sections are shown for the middle horizontal line of 2D images: solid ('red') for reconstructions and dotted ('blue') for true variables.

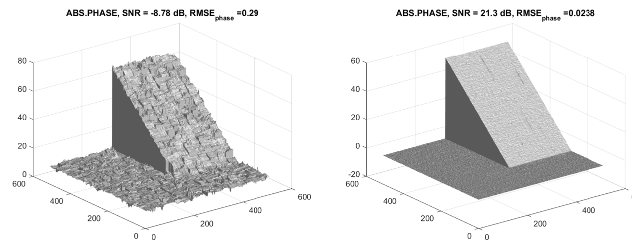


Fig. 5. Sub-wavelength resolution of share plane absolute phase, maximum value 56.8 rad, $r_s$. Reconstructions from the very noisy data (left, failed) and the nearly noiseless data (right).

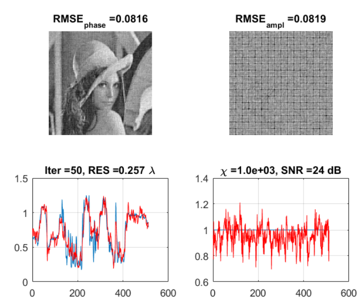


Fig. 6. Super-resolution SPAR Lena phase image reconstructions, $r_s = 32$. The computational pixels are equal to 0.257 $\lambda$, sub-wavelength resolution is shown.

## REFERENCES

[1] R. K. Tyson. *Principles of Adaptive Optics*. 4rd ed., CRC Press, 2014.
[2] Th. Kreis, *Handbook of Holographic Interferometry*. Wiley-VCH, Berlin, 2005.
[3] B. Kress and P. Meyrueis. *Applied Digital Optics: From Micro-Optics to Nanooptics*. John Wiley & Sons, Inc., 2009.
[4] Katkovnik, V., Ponomarenko, M. & Egiazarian, K. "Sparse approximations in complex domain based on BM3D modeling," *http://www.cs.tut.fi/sgn/imaging/sparse/*, 2017.
[5] V. Katkovnik and J. Astola, " High-accuracy wavefield reconstruction: decoupled inverse imaging with sparse modeling of phase and amplitude," *J. Opt. Soc. Am. A*, vol. 29, (2012) 44 – 54.
[6] V. Katkovnik and J. Astola, "Compressive sensing computational ghost imaging," *J. Opt. Soc. Am. A*, vol. 29 no. 8 (2012) 1556-1567.
[7] V. Katkovnik, "Phase retrieval from noisy data based on sparse approximation of object phase and amplitude", *http://www.cs.tut.fi/~lasip/DDT/index3.html.*
[8] C. A. Metzler, A. Maleki, R. G. Baraniuk, "BM3D-PRGAMP: Compressive phase retrieval based on BM3D denoising," *IEEE International Conference on Image Processing (ICIP)*, 2016.
[9] H. Hongxing, J. M. Bioucas-Dias, and V. Katkovnik, "Interferometric phase image estimation via sparse coding in the complex domain," *IEEE Trans. on Geoscience and Remote Sensing*, vol. 53 no. 5 (2015) 2587 - 2602.
[10] V. Katkovnik, K Egiazarian, J. Bioucas-Dias,'Phase imaging via sparse coding in the complex domain based on high-order SVD and nonlocal BM3D techniques,' *Proceedings of IEEE International Conference on Image Processing* (*ICIP 2014*), (2014) 4587-4591.
[11] V. Katkovnik and K. Egiazarian, "Complex domain sparse phase imaging based on nonlocal BM3D techniques", *Digital Signal Processing*, 63, (2017) 72–85.